

# Hollow Cathode Chemical Modelling

M. Coletti and S. B. Gabriel

University of Southampton, Southampton, United Kingdom, SO17 1BJ

## ABSTRACT

In this paper the state of hollow cathode life time modelling at the University of Southampton will be reported. Two models have been developed: one for BaO depletion from the hollow cathode insert and another for low work function compounds deposition and desorption. The model developed to predict BaO depletion from hollow cathode insert will be presented together with some comparison between experimental and numerical data to prove its validity.

A model for low work function compounds deposition and desorption will also be presented. This model will be used to simulate the NSTAR cathode showing a very conservative estimate of the cathode life due to conservative character of the hypotheses made in the model development and due to the chosen criteria for the end of life.

## I. INTRODUCTION

Hollow cathodes are a key component in the electric propulsion field. They are used as electron sources and neutralizers inside ion thruster and Hall's effect thrusters and in the next future probably as stand alone microthrusters [1], [2] therefore their lifetime and performance are key elements in all the application mentioned above.

The performances and the lifetime of hollow cathodes are closely linked to the thermionic emission from the emitter surface.

Hollow cathodes have demonstrated the ability of providing 30000 hours of functioning [3] whereas no experimental data exists above this limit.

The importance of hollow cathode lifetime is a growing issue for deep space mission using propulsive systems based on Ion or Hall effect Thrusters that may require longer lifetimes than those demonstrated up to now or that may require operations at conditions that differ from those of the long duration tests.

To address these concerns about hollow cathode lifetime and to prove the suitability of an ion thrusters based SEP subsystem for future high impulse mission such as the Bepi-Colombo mission QinetiQ and the University of Southampton have started a project to study and model the main processes responsible of lifetime limitation in hollow cathodes.

During normal operation of the cathode the work function of the emitter surface is lowered from the typical value of the emitter material (for tungsten  $\phi = 4.5$  eV) down to about 2 eV thanks to the evaporation of BaO from the emitter core and its subsequent

deposition on the emitting surface resulting in the formation of low work function compounds.

During cathode life the evaporation rate of BaO from the insert tends to decrease due to the gradual depletion of BaO, hence the low work function deposition rates will decrease as well resulting in a reduction of the area covered by low work function compounds and in an increase of the overall work function. This process leads to a reduction of the thermionic current from the emitter up to the point where the cathode is no longer able to operate.

It is then clear how the understanding of the evaporation, deposition and desorption processes involving BaO and the surface low work function compounds are key in predicting the lifetime of the cathode.

In this paper the results obtained up to present at the University of Southampton will be presented. Firstly the chemical model for BaO desorption from a hollow cathode insert will be presented [4] then the model for low work function deposition and desorption will be reported [5].

## II. BARIUM OXIDE DEPLETION MODEL

The barium oxide content inside the insert is depleted due to the effect of BaO evaporation from the insert surface. This evaporation depends on the compounds formed by BaO with CaO and Al<sub>2</sub>O<sub>3</sub> and causes a concentration gradient between the insert surface and the insert core. This gradient will give raise to a diffusion motion that will replenish BaO at the insert surface.

In this model both the dependencies of BaO evaporation rate from the chemistry of the BaO-CaO-Al<sub>2</sub>O<sub>3</sub> system and the diffusion processes bringing BaO from the insert core to the surface will be included.

The chemistry of the BaO-CaO-Al<sub>2</sub>O<sub>3</sub> system will be modeled using the data contained in the ternary diagram reported below

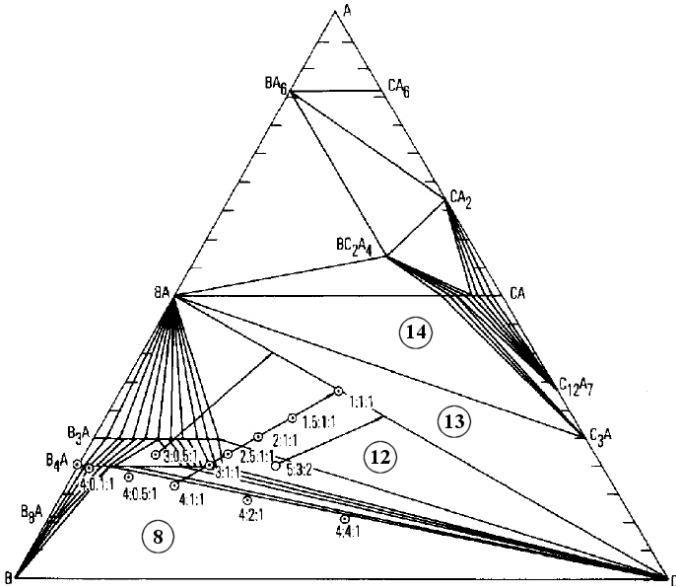


Fig. 1 BaO-CaO-Al<sub>2</sub>O<sub>3</sub> ternary diagram at 1250 °C [6]

In this diagram the letters A, B and C stand for Al<sub>2</sub>O<sub>3</sub>, BaO and CaO respectively. Each of the three corners represents a mass concentration of 100% of one of these three fundamental compounds (the one displayed near the corner).

Each point of the diagram represents a state of the system where the concentration of A, B and C are inversely proportional to the distance of the point from each corner.

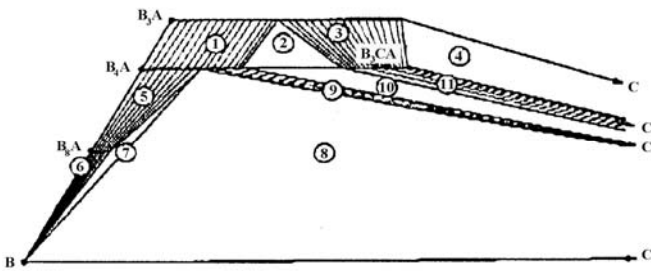


Fig. 2 Particular of the BaO-CaO-Al<sub>2</sub>O<sub>3</sub> ternary diagram [7]

Each of the areas in which the diagram is divided represents a particular state of the system i.e. which compounds are present.

The empty areas stand for states in which the compounds stoichiometric coefficients are fixed while the filled ones stand for states in which the stoichiometric coefficients changes with the composition.

In most of these compounds we can find that the barium oxide can be partially substituted by calcium oxide because of their similar atomic configuration, when this happens we will refer to these compounds as solid solution (s.s.).

Area	Compounds
1	B <sub>3</sub> A s.s. and B <sub>4</sub> A s.s.

2	$\overline{B_3A}$ s.s., $\overline{B_4A}$ s.s. and $\overline{B_3CA}$
3	$\overline{B_3A}$ s.s. and $\overline{B_3CA}$ s.s.
4	C, $\overline{B_3A}$ s.s. and $\overline{B_3CA}$ s.s.
5	$\overline{B_4A}$ s.s. and $\overline{B_8A}$ s.s.
6	B and $\overline{B_8A}$ s.s.
7	B, $\overline{B_4A}$ s.s. and $\overline{B_8A}$ s.s.
8	B, C and $\overline{B_4A}$ s.s.
9	C and $\overline{B_4A}$ s.s.
10	C, $\overline{B_4A}$ s.s. and $\overline{B_3CA}$ s.s.
11	C and $\overline{B_3CA}$ s.s.
12	C, B <sub>3</sub> A and BA
13	C, BA and C <sub>3</sub> A
14	AB, C <sub>3</sub> A and CA

The barred formulae refer to a well-defined composition of the corresponding solid solution. [7], [8]

Once we know which compounds are present and which are their stoichiometric coefficients, using the conservation of atomic species we can calculate the final composition.

For example a 2:1:1 composition (that in mass fraction corresponds to: 50% BaO, 25% CaO, 25% Al<sub>2</sub>O<sub>3</sub>) corresponds to area number 12 of the diagram so the compounds present are C, B<sub>3</sub>A and BA.

Using the conservation of atomic species the final composition is found to be 2C+B<sub>3</sub>A+BA or the equivalent 2CaO+Ba<sub>3</sub>Al<sub>2</sub>O<sub>6</sub>+BaAl<sub>2</sub>O<sub>4</sub>.

Once the exact composition has been determined using the data in Table 2 the barium oxide pressure can be calculated as

$$P_{BaO\ tot} = \sum_{i=1}^N \left( e^{\frac{-q\Delta H_i + \Delta S_i}{kT} + \frac{\Delta S_i}{R}} \cdot 10^5 \cdot X_i \right) \quad (1)$$

where the index *i* is used to label the pressure relative to the *i*-th compound.

Reactions	$\Delta H$ , eV	$\Delta S$ , J/mol
BaO(s)→BaO(g)	4.3224	137.85
1/5 Ba <sub>8</sub> Al <sub>2</sub> O <sub>11</sub> (s) →BaO(g)+ 1/4 Ba <sub>4</sub> Al <sub>2</sub> O <sub>7</sub> (s)	4.4267	130.72
Ba <sub>4</sub> Al <sub>2</sub> O <sub>7</sub> (s) →BaO(g)+Ba <sub>3</sub> Al <sub>2</sub> O <sub>6</sub> (s)	4.5789	122.76
1/2 Ba <sub>3</sub> Al <sub>2</sub> O <sub>6</sub> (s)→BaO(g)+ 1/2BaAl <sub>2</sub> O <sub>4</sub> (s)	4.6615	125.28
6/5BaAl <sub>2</sub> O <sub>4</sub> (s)→BaO(g)+1/5BaAl <sub>12</sub> O <sub>19</sub> (s)	5.6095	124.86
Decomposition of solid solution	$\Delta H$ , eV	$\Delta S$ , J/mol
Ba <sub>8-0.2</sub> Ca <sub>0.2</sub> Al <sub>2</sub> O <sub>11</sub>	4.4267	130.47
Ba <sub>4-1.1</sub> Ca <sub>1.1</sub> Al <sub>2</sub> O <sub>7</sub>	4.5789	122.05
Ba <sub>3-0.75</sub> Ca <sub>0.75</sub> Al <sub>2</sub> O <sub>6</sub>	4.6615	122.93

$\Delta H$  and  $\Delta S$  represent the enthalpy and entropy of the reactions. [6], [9]

From Eq. (1) the mass flow rate can be obtained through the Knudsen-Hertz-Langmuir formula [6]

$$\dot{m}_{BaO} = \frac{P_{BaO_{tot}}}{\sqrt{\frac{2\pi RT}{M_{BaO}}}} \quad (2)$$

Using Eq. (2) and starting from a 4:1:1 composition the evolution of the BaO mass flow rate with the BaO content (assuming constant CaO and Al<sub>2</sub>O<sub>3</sub> content) can be calculated.

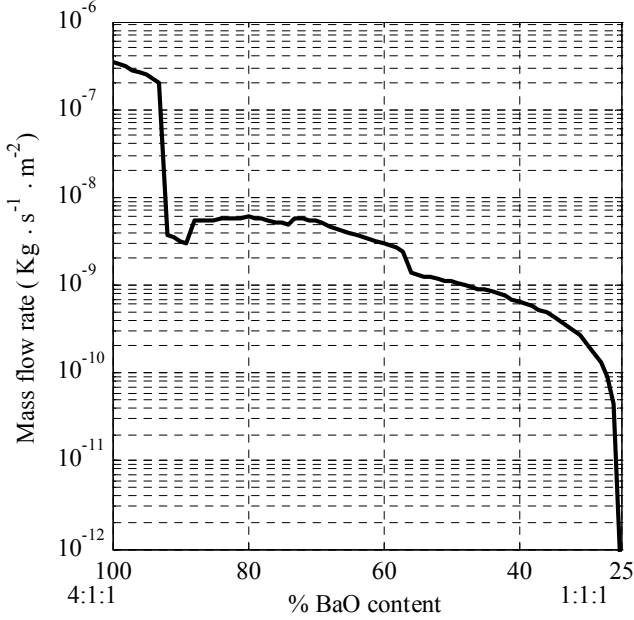


Fig. 3 BaO mass flow rate trend with local BaO content [4]

As it can be seen the mass flow rate trend is strongly non linear showing the importance of the knowledge impregnant composition in the calculation of the BaO evaporation rate.

From the knowledge of the trend of the mass flow rate with barium local concentration a model for barium oxide depletion from the insert can be formulated.

Assuming that all the diffusion processes that concur in bringing BaO from the core of the insert to the surface can be represented with a single diffusion coefficient  $D_a$ , the BaO depletion process from a cylindrical insert can be mathematically described as

$$\frac{\partial \rho}{\partial t} - D_a \left( \frac{1}{r} \frac{\partial \rho}{\partial r} + \frac{\partial^2 \rho}{\partial r^2} + \frac{\partial^2 \rho}{\partial z^2} \right) - \frac{\partial \rho}{\partial z} \frac{\partial D_a}{\partial z} = 0 \quad (3)$$

where  $\rho$  indicates the local BaO density and where at the boundaries the mass flow rate of BaO calculated with Eq. (2) is imposed.

Solving Eq. (3) numerically and performing a sensitivity analysis on the value of the diffusion coefficient to match the computed depletion profiles with those measured by Roquais [10] the trend of the diffusion coefficient with insert temperature ( $T$ ) and porosity ( $IT$ ) has been derived.

$$D_a = (b\Pi + c) e^{-\frac{qE_{Da}}{kT}} \quad (4)$$

$$b = 0.1165 \text{ m}^2 / \text{s}$$

$$c = -0.01653 \text{ m}^2 / \text{s}$$

$$E_{Da} = 3.5 \text{ eV}$$

### III. BARIUM OXIDE DEPLETION MODEL VALIDATION

The model derived in the section before has been validated simulating the T5 Artemis cathode by QinetiQ [11] and the NSTAR cathode from the Deep Space 1 Spare Ion Engine [3].

The T5 Artemis has been successfully tested at QinetiQ accumulating 15000 hours of operation at 2.6 A of discharge current; the test has been terminated voluntarily.

The cathode has then been sectioned and analyzed with EDX technique to derive the profile of BaO depletion.

The results of the analysis of the downstream end of the cathode is reported below

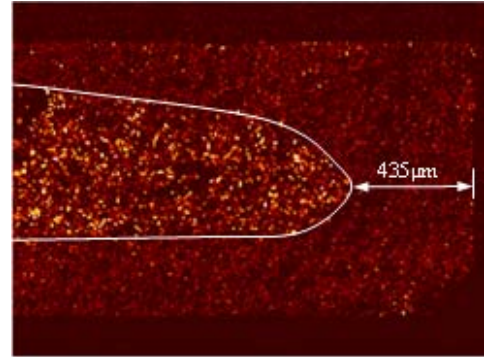


Fig. 4 EDX mapping of Barium L  $\alpha$  line, showing 435  $\mu\text{m}$  of depletion from the downstream face after 15,000 hours of operation [11]

where dark zones represent areas where BaO has been depleted whereas bright area represent undepleted conditions.

The cathode tube has also been inspected finding BaO deposition on its interior surface meaning that BaO evaporation occurs also from the insert external surface.

The T5 cathode has then been numerically simulated for 15000 hours using the measured insert temperature profile and assuming that evaporation occurs from the inner and outer insert surface and from the upstream surface. An initial flat BaO content inside the insert has also been assumed.

The BaO depletion colormap relative to the same region presented in Fig. 4 is reported below where the values on the colormap indicate the local percent of BaO remaining with respect to the initial value (1 means that no BaO has been depleted, 0 means all the BaO has been depleted).

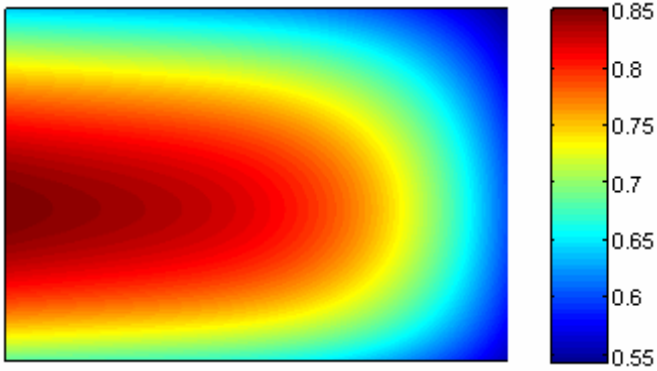


Fig. 5 Simulated BaO depletion profile

Unfortunately the data reported in Fig 4 are only qualitative since no absolute data relative to the BaO content has been reported. Hence only a qualitative comparison is possible.

The comparison between the experimental depletion profile derived from Fig 4 (white line) and the best fitting iso-depletion line from Fig 5 (blue line) is reported below.

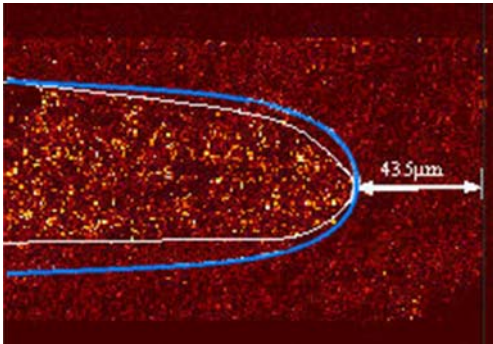


Fig. 6 Direct comparison between experimental and numerical results

The agreement between the iso-depletion line and the experimental depletion profile is satisfactory with the iso-depletion line following the experimental result very closely in his top part.

The NSTAR cathode has also been simulated using the temperature profile reported in Ref [12].

The NSTAR cathode has been tested for 30000 hours. The test has been voluntary interrupted and the cathode has then been sectioned and analyzed [3].

This cathode has been simulated assuming a series of different boundary conditions and assuming gaps between the outer insert surface and the cathode tube of 25, 50, 75 and 100  $\mu\text{m}$ . The best result has been obtained assuming BaO evaporation to occur form all the insert surfaces except the orifice plate surface and assuming that the gap between the outer insert surface and the cathode tube is 75  $\mu\text{m}$  [13].

The comparison between numerical and experimental data is reported below.

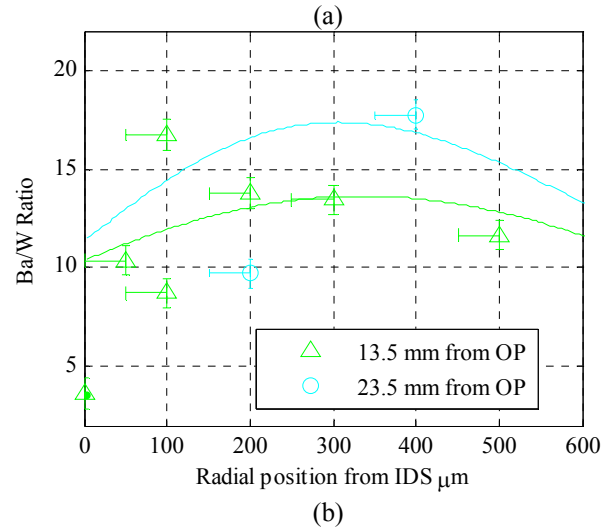
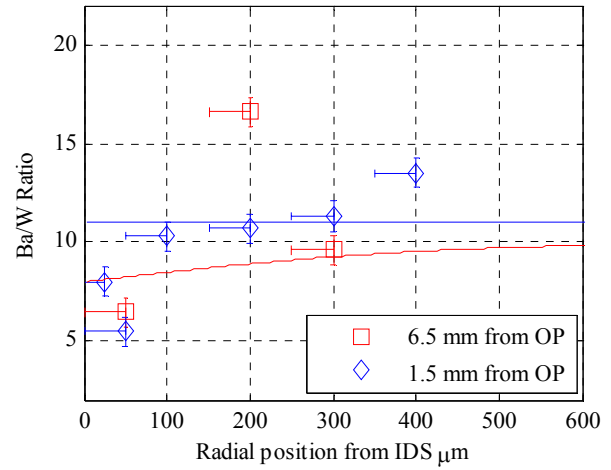


Fig. 7 – Comparison between numerical and experimental BaO depletion values. (a) downstream end (b) upstream end[13]

where OP and IDS stand respectively for orifice plate and internal diameter surface.

As it can be seen from Fig. 7 there is a good quantitative agreement between experimental and theoretical data.

The numerical results relative to 1.5 mm in Fig 7 (a) show a flat profile with a value close to the average of the measured values. The fact that the computed profile is flat is due to the high temperature in the downstream region that, increasing the value of the diffusion coefficient, tends to “flatten” the depletion profile.

The fact that the experimental profile does not show the same flat trend could be due to W deposition on the downstream end that, chugging the insert pores, will hinder BaO evaporation.

Regarding the data relative to 6.5 mm from the OP it can be noted that the experimental trend is quite unusual showing a peak of barium content at one quarter of the insert thickness. If we neglect the point relative to 6.5 mm from the OP and to 200  $\mu\text{m}$  from the IDS the computed data are in good agreement with the experimental ones.

Looking at the data relative to 13.5 and 23.5 mm from the OP we can note how they show a good agreement with the experimental measurement.

In conclusion the model developed to simulate BaO depletion from hollow cathode inserts is able to produce numerical results that are both in qualitative and quantitative agreement with the experimental measurement including both the dependence of the mass flow rate from the local BaO content and the diffusion motion of BaO inside the insert.

#### IV. LOW WORK FUNCTION COMPOUNDS DEPOSITION AND DESORPTION MODELLING

After the BaO depletion from the hollow cathode insert has been successfully modelled a model for the low work function compounds deposition and desorption on the insert surface has been developed. Before developing such a model the chemistry of the system composed by tungsten, barium, calcium and oxygen will be qualitatively presented starting from the data in Ref [14], [17] and [18]. The work function of the most important barium-tungsten compounds have been studied by Bondarenko [14] and are reported below

$$\phi = \phi_0 + \frac{d\phi}{dT} T \quad (4)$$

BaO:WO <sub>3</sub>	Compound	$\phi$ [eV] T=1100°C	$\phi_0$ [eV]	$\frac{d\phi}{dT}$ [eV·K <sup>-1</sup> ]
5 : 1	Ba <sub>3</sub> WO <sub>6</sub>	2.00	1.33	$6.09 \cdot 10^{-4}$
3 : 1	Ba <sub>3</sub> WO <sub>6</sub>	2.42	1.02	$12.72 \cdot 10^{-4}$
2 : 1	Ba <sub>2</sub> WO <sub>5</sub>	2.76	1.85	$8.27 \cdot 10^{-4}$
1 : 1	BaWO <sub>4</sub>	3.34	2.27	$9.72 \cdot 10^{-4}$

The hollow cathode overall work function trend with temperature has been reported to be [15]

$$\phi = 1.41 + 5 \cdot 10^{-4} T \quad (5)$$

This trend is very close to the one of Ba<sub>3</sub>WO<sub>6</sub> relative to the highest BaO content.

If we consider that in normal conditions a cathode will operate at temperature below 1300 °C the maximum difference between the work function measured at JPL [15] and the one relative to Ba<sub>3</sub>WO<sub>6</sub> is about 0.1 eV equivalent to the 4% of the measured value.

From this we can infer that this is the compound responsible for work function lowering on a hollow cathode emitter surface. This is in agreement with the observation made by Sarver-Verhey [16] where Ba<sub>3</sub>WO<sub>6</sub> has been found in the “active” area of the emitter surface.

To understand how this compound is formed and its resistance to temperature we will refer to the phase diagrams presented in Fig. 8-10.

The phase diagrams of all the possible combination of tungsten, oxygen, tungsten oxide, barium oxide and calcium oxide are presented below

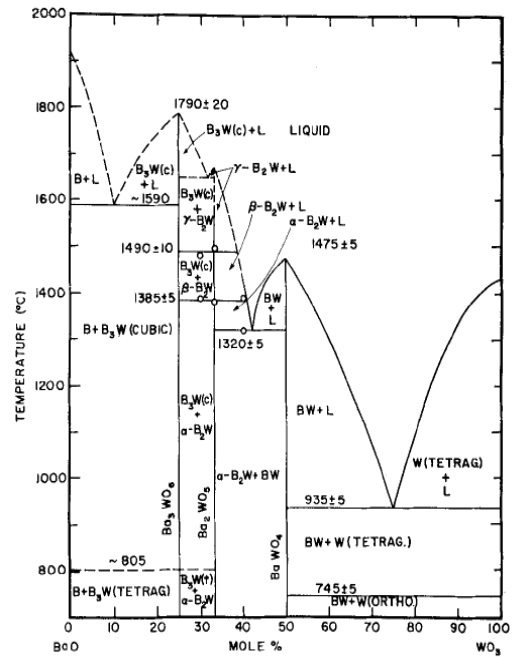


Fig. 8 Phase diagram BaO-WO<sub>3</sub> [17]

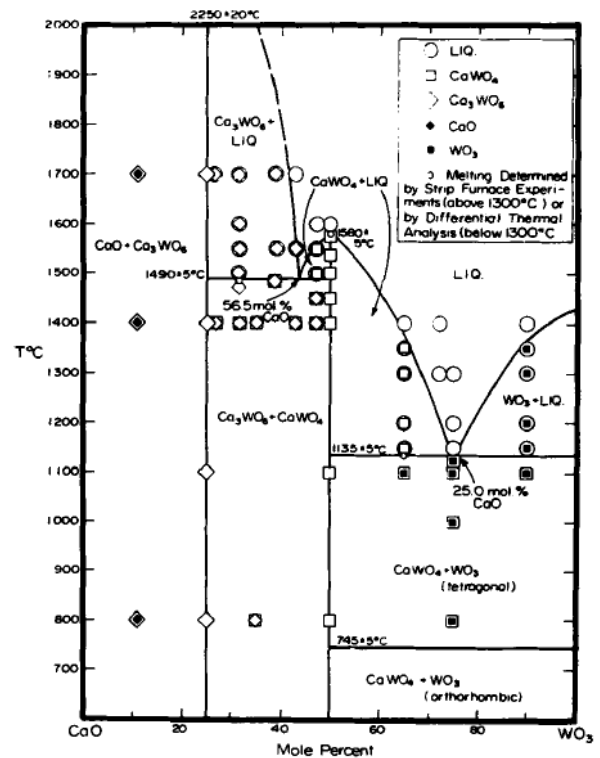


Fig. 9 Phase diagram CaO- WO<sub>3</sub> [18]

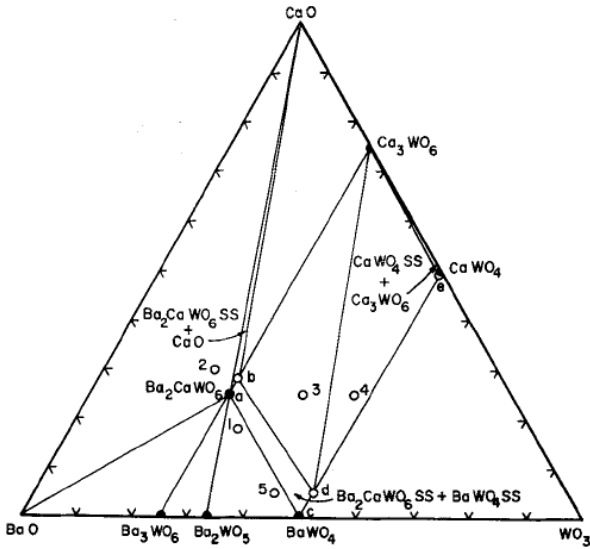


Fig. 10 Phase diagram BaO-CaO-WO<sub>3</sub> section at 1200°C [17]

Looking at Fig. 8 Ba<sub>3</sub>WO<sub>6</sub> seems to be stable up to 1600 °C. In spite of this in Ref [9] it has been found that Ba<sub>3</sub>WO<sub>6</sub> does not evaporate directly but tend to decompose in BaWO<sub>4</sub> and then this dissociates in WO<sub>3</sub> and gaseous BaO at about 1500 °C.

These temperatures are far above the normal working temperatures of a cathode and, in fact, later it will be shown that the main low work function compounds desorption mechanism is not thermal evaporation but ion bombardment.

The reaction involving Ba<sub>3</sub>WO<sub>6</sub> and BaWO<sub>4</sub> are reported below [7], [9].

Reaction	$\Delta H$ [eV]	$\Delta S$ [kJ/mol]
$Ba_3WO_6(s) \Leftrightarrow 2BaO(g) + BaWO_4(s)$	11.39	320.11
$BaWO_4(s) \Leftrightarrow BaO(g) + WO_3(s)$	12.34	137.98

Where the BaO pressure (in atmospheres), that is directly proportional to the Ba<sub>3</sub>WO<sub>6</sub> / BaWO<sub>4</sub> desorption rate, produced by these reactions can be expressed as

$$p_{BaO} = e^{\left(\frac{\Delta H}{kT} + \frac{\Delta S}{R}\right) \frac{1}{\xi_{BaO}}} \quad (6)$$

and where  $\xi_{BaO}$  represents the stoichiometric coefficient of BaO in the reactions.

Looking at Fig. 8, 9 a strong similarity between the two phase diagrams can be found. BaO and CaO tend to form exactly the same kind of compounds with WO<sub>3</sub> because of their similar atomic structure. The only difference is that the compounds formed by CaO have a much higher resistance to temperature.

Looking at Fig. 10 is possible to see how solid solution between BaO and CaO compounds can occur with partial substitution of barium oxide with calcium oxide.

The work functions of calcium-tungsten compounds have not been found in the literature.

Considering the similarities in atomic structure and work function between calcium and barium it is safe to assume that the work functions of the solid solutions Ba<sub>3-x</sub>Ca<sub>x</sub>WO<sub>6</sub> and Ba<sub>1-x</sub>Ca<sub>x</sub>WO<sub>4</sub> will not be sensibly different from the ones relative to Ba<sub>3</sub>WO<sub>6</sub>, BaWO<sub>4</sub> reported in Table 3.

From these observations the presence of CaO inside the impregnate can be justified as follows.

BaO is a low work function compound that evaporates at relatively low temperatures, once evaporated it deposits on the tungsten surface creating low work function compounds (mainly Ba<sub>3</sub>WO<sub>6</sub>) whereas CaO evaporation rate is much lower and its compounds can resist to much higher temperatures than the BaO ones. Therefore a partial substitution of BaO with CaO will generate high temperature resistant low work function compounds.

The function of BaO is, thanks to its relatively high evaporation rates, to provide the “base material” needed to build as many low work function compounds as possible; the function of CaO is, substituting a small fraction of BaO, to give to these compounds resistance to temperature.

Considering all this the usual 4:1 ratio between BaO and CaO can be qualitatively explained.

#### Deposition Modelling

Deposition of barium on the emitter surface is the results of the reactions reported in Table 4 when these proceed from right to left. To predict the exact behaviour of deposition with time the forward and backward reactions constants would be needed. Unfortunately these data has not been found in the literature; the only data available are relative to the equilibrium constant of the reactions.

From the definition of equilibrium constant we have

$$K_p = \frac{k_f}{k_b} = e^{-\frac{\Delta H}{kT} + \frac{\Delta S}{R}} \quad (7)$$

Hence if  $K_p \gg 1$  the reaction will be shifted to the right whereas if  $K_p \ll 1$  the reaction will be shifted to the left. The values of the  $K_p$  are reported in Table 5

Reaction	$K_p$	
$Ba_3WO_6(s) \Leftrightarrow 2BaO(g) + BaWO_4(s)$	$8.91 \cdot 10^{-26}$	$k_f \ll k_b$
$BaWO_4(s) \Leftrightarrow BaO(g) + WO_3(s)$	$8.95 \cdot 10^{-39}$	$k_f \ll k_b$

As can be seen in Table 5 the equilibrium constant for these two reactions are very small meaning that the reactions are completely shifted to the left. From this we can infer that barium oxide react with tungsten very easily and quickly to form BaWO<sub>4</sub> and then Ba<sub>3</sub>WO<sub>6</sub>.

Based on this we can formulate the hypothesis that all the barium oxide that evaporates from the insert deposits on the emitter surface creating Ba<sub>3</sub>WO<sub>6</sub>. From this assumption the deposition rate of low work function compounds per unit area is

$$\dot{N}_{Ba_3WO_6}^+ = \frac{1}{3} \Pi \frac{\dot{m}_{BaO}}{m_{BaO}} \quad (8)$$

Where  $\dot{m}_{BaO}$  is the mass flow rate of BaO from the insert per unit area calculated from the chemical model in Sec. II.

### Desorption Modelling

Desorption of low work function compounds is the results of the reactions reported in Table 4 when these proceed from left to right. As shown before the equilibrium constant of these reactions is very small hence we will expect the desorption rates due to thermal evaporation to be really low.

Using Eq. 6 the desorption rates per unit area relative to thermal evaporation are

$$\dot{N}_{Ba_3WO_6}^{-th} = \frac{1}{2} g(1-\Pi) e^{\left(\frac{-\Delta H + \Delta S}{kT} + \frac{\Delta S}{R}\right) \frac{1}{2}} \frac{10^5}{m_{BaO} \sqrt{\frac{2\pi RT}{M_{BaO}}}} \quad (9)$$

$$\dot{N}_{BaWO_4}^{-th} = g(1-\Pi) e^{\left(\frac{-\Delta H + \Delta S}{kT} + \frac{\Delta S}{R}\right)} \frac{10^5}{m_{BaO} \sqrt{\frac{2\pi RT}{M_{BaO}}}} \quad (10)$$

A comparison between this two desorption rates is presented in Table 6.

Compound	900°C	1000°C	1100°C	1200°C
Ba <sub>3</sub> WO <sub>6</sub>	2.69·10 <sup>10</sup>	2.14·10 <sup>12</sup>	9·10 <sup>13</sup>	2.27·10 <sup>15</sup>
BaWO <sub>4</sub>	9.71·10 <sup>-20</sup>	1.35·10 <sup>-15</sup>	4.6·10 <sup>-12</sup>	5.32·10 <sup>-9</sup>

As can be seen the BaWO<sub>4</sub> desorption rates are smaller than the ones relative to Ba<sub>3</sub>WO<sub>6</sub> and are also smaller than unity meaning that BaWO<sub>4</sub> desorption is absolutely negligible since it will take more than one second to remove one low work function molecule per meter squared.

Another important desorption mechanism is ion bombardment from the hollow cathode plasma. This desorption rate can be written as

$$\dot{N}^{-bomb} = n_i v_{th} (1-\Pi) g Y_{sputt} \quad (11)$$

Where  $v_{th}$  is the sputtered particle thermal velocity that can be expressed as

$$v_{th} = \sqrt{\frac{kT}{2\pi m}} \quad (12)$$

and  $Y_{sputt}$  is the sputtering yield of Ba<sub>3</sub>WO<sub>6</sub> or BaWO<sub>4</sub>. Unfortunately no data regarding the sputtering yield of

these two compounds have been found in the literature.

The theories that are commonly used to calculate the sputtering yield are based on data that are currently unknown for these compounds like surface binding energy and collision cross sections.

The sputtering yield will be then calculated starting from the theory developed by Langmuir[19].

In this theory the sputtering process is explained as follows: "...an ion striking on the cathode surface will drive the cathode atom it strikes into the surface creating a local depression..." the ion is then been reflected and after the reflection "the ion may have enough momentum to knock off a cathode atom around the edge of the depression" [19].

Starting from this and applying the conservation of kinetic energy and the conservation of momentum to the first and the second collision Langmuir found that the energy transferred by the impacting ion to the cathode atom in the second collision is

$$E_{trans} = \alpha E_0 \quad (13)$$

Where  $E_0$  is the initial kinetic energy of the impacting ion and  $\alpha$  is a coefficient defined as follows

$$\alpha = 4 m_c m_g \left[ \frac{m_g - m_c}{(m_g + m_c)^2} \right]^2 \quad (14)$$

Where  $m_c$  and  $m_g$  are respectively the mass of the impacting ion and of the cathode molecule.

Once we know the energy transferred from the ion to the cathode surface the probability that a cathode atom is sputtered is related to the ratio between the activation energy needed for the cathode atom evaporation process and the energy transferred by the impacting ions.

If the energy of the impacting ions is of the order of some eV the sputtering yield will certainly be smaller than unity hence we can assume  $Y_{sputt}$  to be equal to the exponential of the ratio between the activation energy and the energy transferred to the cathode surface.

In formula

$$Y_{sputt} = e^{-\frac{E_{act}}{E_{trans}}} = e^{-\frac{E_{act}}{\alpha E_0}} \quad (15)$$

The activation energies of the decomposition processes relative to Ba<sub>3</sub>WO<sub>6</sub> and BaWO<sub>4</sub> are unknown. These energies are certainly higher than the free Gibbs energies [20] relative to the reactions reported in Table 4 hence the assumption

$$E_{act} = \Delta G = \Delta H - T\Delta S \quad (16)$$

will produce higher values of the sputtering yield and of the desorption rates therefore giving a conservative estimation on the low work function surface coverage evolution.

So substituting Eq. 15 and 16 into Eq. 11 and assuming that the voltage drop is much higher than the ion temperature expressed in eV we get the final expression of the sputtering related desorption rate

$$\dot{N}^{-bomb} = n_i v_{th} (1 - \Pi) \mathcal{G} e^{-\frac{E_{act}}{\alpha \Delta V_{sheath}}} \quad (17)$$

As already done with the thermal desorption rate we can compare the sputtering ones for Ba<sub>3</sub>WO<sub>6</sub> and BaWO<sub>4</sub>. The results are reported in Table 7

$n_i$	$\Delta V_{sheath}$	$\Pi$	$\mathcal{G}$
10 <sup>20</sup>	5 V	80%	1
Compound	1000 °C	1100 °C	1200 °C
Ba <sub>3</sub> WO <sub>6</sub>	7.21 · 10 <sup>19</sup>	9.7 · 10 <sup>19</sup>	1.32 · 10 <sup>20</sup>
BaWO <sub>4</sub>	2.32 · 10 <sup>17</sup>	2.82 · 10 <sup>17</sup>	3.42 · 10 <sup>17</sup>

As we can see also in this case the desorption rates relative to BaWO<sub>4</sub> are much smaller than the one relative Ba<sub>3</sub>WO<sub>6</sub>. The implication of this will be discussed later.

#### Insert low work function coverage calculation

From the analysis of the deposition and desorption rates the calculation of the low work function compound surface coverage and of the effective insert work function can be carried out.

Assuming that for a full coverage every tungsten atom that was originally on the surface is bonded with barium and oxygen to form Ba<sub>3</sub>WO<sub>6</sub> the rate of change of the surface coverage can be expressed as

$$\dot{\mathcal{G}} = \frac{m_W}{\sigma_W} \left[ \dot{N}_{Ba_3WO_6}^+ - \left( \dot{N}_{Ba_3WO_6}^{-th} + \dot{N}_{Ba_3WO_6}^{-bomb} \right) \right] \quad (18)$$

Where  $m_W$  and  $\sigma_w$  are the atomic mass and the surface density of tungsten.

In Eq. 18 the desorption rates of BaWO<sub>4</sub> have been neglected considering they are at least two order of magnitude smaller than the one relative to Ba<sub>3</sub>WO<sub>6</sub>.

Equation 18 can be rewritten as follows

$$\dot{\mathcal{G}} = X\mathcal{G} + Y \quad (19)$$

The evolution of  $\mathcal{G}$  with time can be then calculated analytically as

$$\mathcal{G}(t) = e^{\int_0^t X(\tau) d\tau} \left( \mathcal{G}(0) + \int_0^t Y(\tau) e^{-\int_0^\tau X(\tau) d\tau} d\tau \right) \quad (20)$$

The value of  $\mathcal{G}$  so found is relative to the coverage of the tungsten surface of the insert, we must consider that also the BaO present in the pores will contribute in lowering the average work function hence the effective surface coverage will be

$$\mathcal{G}_{eff}(t) = (1 - \Pi) \mathcal{G}(t) + \Pi \rho_{BaO}(t) \quad (21)$$

Where  $\rho_{BaO}$  is the BaO relative density inside the pores and is one of the outputs of the chemical model described in Sec II.

Once the value of  $\mathcal{G}_{eff}$  is known the work function can be calculated using the formula proposed by Longo [21] including the Schottky effect

$$\phi(\mathcal{G}_{eff}) = \phi_m \left( \frac{\Gamma \phi_m}{\phi_{Ba}} \right)^{\frac{\Gamma \mathcal{G}_{eff}}{1-\Gamma}} + \phi_{Ba} \left[ 1 - \left( \frac{\Gamma \phi_m}{\phi_{Ba}} \right)^{\frac{\mathcal{G}_{eff}}{1-\Gamma}} \right] - \sqrt{\frac{qE_w}{4\pi\epsilon_0}} \quad (22)$$

Where  $\phi_m$  is the bare metal (maximum) work function,  $\Gamma$  is a coefficient determined finding the zero of the first derivative of Eq. 22 given the minimum work function (Eq. 5), and where  $E_w$  is calculated according to Siegfried and Wilbur[22].

#### ELT discharge cathode simulation

The model developed up to now will be tested on the NSTAR cathode from the Deep Space 1 Spare Ion Engine. The insert chemistry of this cathode has been already successfully simulated as shown in Sec. III. During the extend life test the discharge cathode has been used at different throttle levels as reported in Table 8

TH level	Accumulated hours	Discharge Current
12	500	9.9
15	4800	13.5
8	10500	7.6
15	15500	13.5
0	21500	4.9
15	25500	13.5
5	30000	6.9

To simulate the cathode the values of  $\Delta V_{sheath}$ ,  $T_w$ ,  $\phi_m$  and  $n_i$  for each TH level and their evolution with time are needed.

The maximum work function value  $\phi_m$  will be set equal to the work function of BaWO<sub>4</sub> reported in Table 3. This will be justified later on.

The values of the plasma parameters, when possible, will be taken from the literature (Ref. [23]-[27]) when these are not available they will be derived from the published data scaling the plasma parameters so that the heat balance equation at the cathode surface is satisfied and the total current flowing to the cathode surface will be equal to the nominal value of the discharge current.

To do so two different hypotheses will be used: constant ion density among all the TH levels or constant  $\Delta V_{sheath}$ .

The cathode has then been simulated for 31000 hours assuming that the initial surface coverage is equal to one.

The surface coverage and work function for different times and for the two different hypotheses are reported below

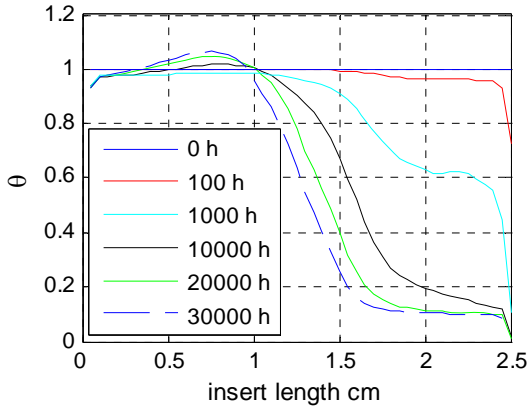


Fig. 11 Surface coverage along the insert for different times assuming  $\Delta V_{sheath} = const$

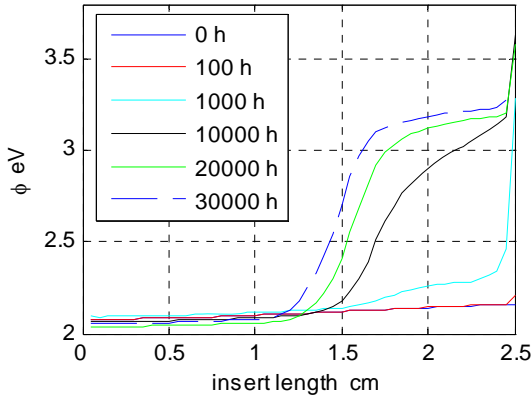


Fig. 12 Work function along the insert for different times assuming  $\Delta V_{sheath} = const$

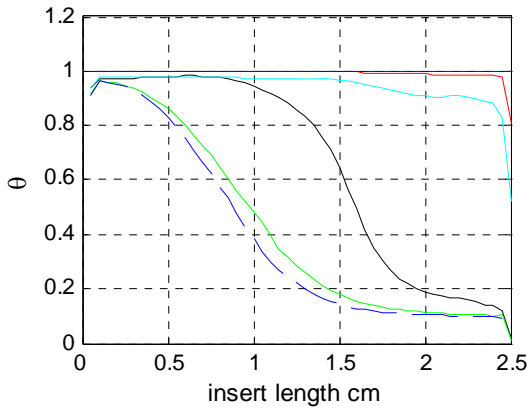


Fig. 13 Surface coverage along the insert for different times assuming  $n_i = const$

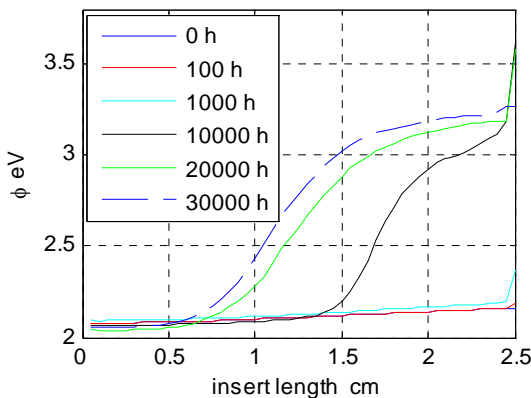


Fig. 14 Work function along the insert for different times assuming  $n_i = const$

As can be seen from Fig 11 and 13 the time needed to have a spot on the insert where all the  $Ba_3WO_6$  has been removed is not shorter than 1000 hours. Noting that the desorption rates for  $BaWO_4$  are about 100 times smaller than the ones relative to  $Ba_3WO_6$ , as reported in Table 7, we can safely state that  $BaWO_4$  removal will happen only on much larger timescales (hundreds of thousands of hours).

Therefore the possibility of having areas of the insert where no low work function compound exists (neither  $Ba_3WO_6$  nor  $BaWO_4$ ) is really small hence the assumption according to which the maximum value of the work function of the insert can be set equal to the value relative to a full coverage of  $BaWO_4$  can be justified.

Looking at the figures above it can be seen how the surface coverage of low work function compounds decrease with time almost everywhere on the cathode surface. It can also be noted from the  $\mathcal{G}$  profiles at the beginning of life and after 10000 hours, and after 20000 and 3000 hours how this process tends to slow down with time.

Looking at the work function evolution it must be noted that, even when all the  $Ba_3WO_6$  has been depleted the work function value is still below 3.5 eV thanks to the remaining  $BaWO_4$  on the surface and thanks to the barium oxide content inside the pores.

Regarding the difference between the two hypotheses made to derive the plasma parameters ( $n_i = const$  and  $\Delta V_{sheath} = const$ ) it can be seen how with the first one the evolution of  $\mathcal{G}$  and  $\phi$  presents a smooth trend along the insert length with higher work function (lower coverage) downstream that gradually decreases (increase) moving upstream; whereas the second hypothesis produces a trend where the downstream of the insert is characterized by a low coverage (high work function) while the upstream region presents an high coverage (low work function) and where the transition between this two region is quite sharp.

From the calculated trend of the surface coverage and work function the thermionically emitted current evolution with time can be calculated.

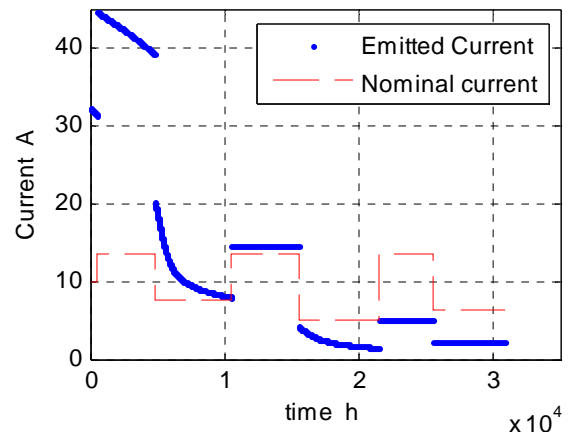


Fig. 15 Emitted and nominal current with time assuming  $n_i = const$

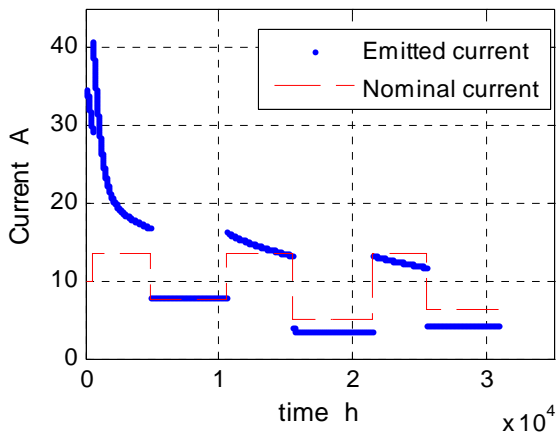


Fig. 16 Emitted and nominal current with time  
 $\Delta V_{sheath} = const$

As it can be noted in both Fig. 15, 16 the emitted current drops below the nominal one after about 15000 hours. If this is taken as a criteria for the hollow cathode end of life the lifetime prevision so obtained is very conservative. This can be explained noting the many conservative assumptions made and noting the fact that chemical model presented in Sec II at present does not take into account CaO evaporation hence neglecting the increase in temperature resistance of the low work function compounds due to the partial substitution of BaO with CaO.

However the fact that the emitted current drops below the cathode nominal current does not necessarily mean that the cathode is not any more able to provide the required current (resulting in a cathode failure) since ion reduction at the cathode wall and secondary emission could provide a significant fraction of the total current.

## V. CONCLUSIONS AND FUTURE WORKS

In the last two years a model for BaO depletion from hollow cathodes insert and low work function deposition and desorption of insert surfaces has been derived at the University of Southampton.

The BaO depletion model takes into account both the chemistry of BaO-CaO- $Al_2O_3$  system and its influence on the BaO evaporation rate, and the diffusion motion of BaO inside the insert.

The model has been compared to the experimental data relative to the T5 Artemis cathode from QinetiQ and to the NSTAR cathode from the Deep Space One Spare Ion Engine showing both a qualitative and a quantitative agreement between the numerical and the experimental measurements.

A low work function compounds desorption and deposition model has also been developed starting from data found in the literature about the chemistry of the Ba-Ca-W system. The processes involved in BaO deposition and desorption have been described and quantified as well as possible (given the chemical data

present in the literature) producing a simple model for deposition and desorption.

Barium oxide has been found to react very quickly with the tungsten surface suggesting the assumption that all the evaporated barium oxide from the insert goes to form low work function compounds.

Two different desorption mechanism have been studied: thermal desorption and ion sputtering. The influence of thermal desorption mechanism has been found to be several order of magnitude lower than that of ion sputtering hence stressing the importance of the knowledge of the plasma parameters evolution relatively to the low work function surface coverage changes.

Once the desorption and deposition rates have been derived a surface coverage model has been formulated and analytically solved.

The model has then been tested with the NSTAR cathode. Assuming that the end-of-life of a cathode occurs when the thermionic current from the emitter surface drops below the nominal current imposed to the cathode by the power supply the life time predicted by this model is of about 15000 hours.

This prevision is very conservative since the NSTAR cathode has demonstrated 30000 hours in ground testing; this has been explained noting the conservative character of assumptions made.

It must also be noted how, to improve the lifetime prediction, an ignition model will be needed since the end of the life of a cathode is normally identified with the impossibility of starting it within the power supply capabilities.

Since the most important desorption mechanism has been found to be ion bombardment from the plasma to improve the accuracy of the model a plasma solver might be coupled to the deposition/desorption calculations to include the effects that a variation in the surface coverage will have on the plasma characteristic.

A life time model able to include both the plasma characteristics change due to surface coverage evolution and a description of the ignition process is currently under development at the University of Southampton.

## REFERENCES

- [1] P. Gessini, M. Coletti, A. Grubisic S. Gabriel, N. Wallace, D. Fearn, "Hollow Cathode Thruster for All-Electric Spacecraft", AIAA-2007-5195, 43rd AIAA/ASME/SAE/ASEE Joint Propulsion Conference & Exhibit, Cincinnati, July 2007.
- [2] M. Coletti, A. Grubisic, N. Wallace, "European Student Moon Orbiter Solar Electric Propulsion Subsystem Architecture. An All - Electric Spacecraft", 30th International Electric Propulsion Conference, Florence, Italy, September 2007.
- [3] A. Sengupta, "Destructive Physical Analysis of Hollow Cathodes from the Deep Space 1 Flight Spare Ion Engine 30,000 Hr Life Test", IEPC-2005-026, Princeton, November 2005
- [4] M. Coletti, S.B. Gabriel, "A Chemical Model for Barium Oxide Depletion from Hollow Cathode's Insert", AIAA-2007-5193, 43rd AIAA/ASME/SAE/ASEE Joint Propulsion Conference & Exhibit, Cincinnati, Ohio, USA, July 2007
- [5] M. Coletti, S.B. Gabriel, "A Model for Low Work Function Compound Deposition on Hollow Cathode Insert Surface", 46th

- AIAA Aerospace Sciences Meeting and Exhibit, Reno, Nevada, USA, January 2008
- [6] R.A. Lipeles, H.K.A. Kan, “*Stability of Barium Calcium Aluminate*”, App. of Surf. Sc., pp16-189, 1983
- [7] P. Appendino, “*Ricerche sul Sistema Ternario Calce-Ossido di Bario-Allumina*”, Ceramurgia, pp. 103-106, 1972.
- [8] G.M Wolten, “*An Appraisal of the Ternary System BaO-CaO-Al<sub>2</sub>O<sub>3</sub>*”, SD-TR-80-67, Space Division, Air Force Command, Los Angeles, 1980
- [9] T.N. Resulhina, V.A. Levitskii, M.Ya. Frenkel, Izvestiya Akademii Nauk SSSR, Neorgan. Mater. 2, pp. 325-331, 1966.
- [10] J.M. Roquais, F. Poret, R. le Doze et al., “*Barium Depletion Study on Impregnated Cathodes and Lifetime Prediction*”, Applied Surface Science 215, pp 5-17, 2003.
- [11] I.M. Ahmed Rudwan, N. Wallace, M. Coletti, S.B. Gabriel, “*Emitter Depletion measurement and modelling in the T5&T6 Kaufman-type Ion Thrusters*”, IEPC-2007-256, 30th Electric International Propulsion Conference, Florence, Italy, September 2007.
- [12] J. Polk, A. Grubisic, N. Taheri, D. Goebel, R. Downey, S. Hornbeck, “*Emitter Temperature Distributions in the NSTAR Discharge Hollow Cathode*”, AIAA-2005-4398
- [13] M. Coletti, A. Grubisic, S.B. Gabriel, “*Numerical Simulation of the Insert Chemistry of the Hollow Cathodes from the Deep Space 1 Ion Engine 30,000 Hrs Life Test*”, IEPC-2007-113, 30th Electric International Propulsion Conference, Florence, Italy, September 2007.
- [14] B.V. Bondarenko, E.P. Ostapchenko, B.M. Tsarev, “*Thermionic Properties of Alkali Metal Tungstates*”, Radiotekh. Elektron, Vol 5, 1960, pp 1246-1253
- [15] I. Mikellides, D. Katz, D. Goebel and J. Polk, “*Model of Hollow Cathode Insert Plasma*”, AIAA-2004-3817, 40th AIAA/ASME/SAE/ASEE Joint Propulsion Conference and Exhibit, Fort Lauderdale, Florida, July 11-14, 2004
- [16] T. R. Sarver-Verhey, “*Destructive Evaluation of a Xenon Hollow Cathode After a 28,000 Hour Life Test*”, NASA/CR—1998-208678, 1998
- [17] E.R. Kreidler, “*Phase Equilibria in the System CaO – BaO – WO<sub>3</sub>*”, Journal of the American Ceramic Society, Vol 55, n 10, 1972, pp 514-519
- [18] L.L.Y. Chang, M.G. Scroger, B. Phillips, “*Alkaline-Earth Tungstates: Equilibrium and Stability in the M – W – O Systems*”, Journal of the American Ceramic Society, Vol 49, n 7, 1966, pp 385-390
- [19] H. Kingdon, I. Langmuir, “*The Removal of Thorium from the Surface of a Thoriated Tungsten Filament by Positive Ion Bombardment*”, Physical review, 1923
- [20] P. Silvestroni, “*Fondamenti di Chimica*”, Veschi Editore, Roma, 1974
- [21] R.T. Longo, “*Physics of Thermionic Dispenser Cathode Aging*”, Journal of Applied Physics, Vol 94, No 10, 2003
- [22] D.E. Sigfried, P.J. Wilbur “*A Model for Mercury Orificed Hollow Cathodes: Theory and Experiment*” AIAA Journal, Vol. 22, No. 10, October 1984
- [23] I. Katz, J. E. Polk, I. G. Mikellides et al. , “*Combined Plasma and Thermal Hollow Cathode Insert Model*”, IEPC-2005-228, 2005.
- [24] I.G. Mikellides, I. Katz, D.M. Goebel, “*Numerical Simulation of the Hollow Cathode Discharge Plasma Dynamics*”, IEPC-2005-200, 2005
- [25] D.M. Goebel, K. Jameson, I. Katz, I.G. Mikellides, “*Energetic Ion Production and Keeper Erosion in Hollow Cathode Discharges*”, IEPC-2005-266, 2005
- [26] I.G. Mikellides , I. Katz, D.M. Goebel, J.E. Polk, “*Hollow Cathode Theory and Experiment. A Two-Dimensional Model of the Emitter Region*”, J. of App. Physics, v98, 2005
- [27] I.G. Mikellides , I. Katz, D.M. Goebel, J.E. Polk, “*Theoretical Model of a Hollow Cathode Plasma for the Assesment of Insert and Keeper Lifetimes*”, 41<sup>st</sup> AIAA Joint Propulsion Conference, Arizona, 2005